



## Proton and helium spectra from the CREAM-III flight

Y. S. YOON<sup>1,2</sup>, H. S. AHN<sup>1</sup>, T. ANDERSON<sup>3</sup>, A. BARRAU<sup>4</sup>, R. BAZER-BACH<sup>5</sup>, J. J. BEATTY<sup>6</sup>, T. J. BRANDT<sup>6</sup>, M. BUÉNERD<sup>4</sup>, N. B. CONKLIN<sup>3</sup>, S. COUTU<sup>3</sup>, L. DEROME<sup>4</sup>, M. A. DUVERNOIS<sup>3</sup>, M. GESKE<sup>3</sup>, J. H. HAN<sup>1</sup>, J. A. JEON<sup>7</sup>, K. C. KIM<sup>1</sup>, M. H. KIM<sup>1</sup>, M. H. LEE<sup>1</sup>, S. E. LEE<sup>1</sup>, J. T. LINK<sup>8,9</sup>, A. MALININ<sup>1</sup>, M. MANGIN-BRINET<sup>4</sup>, A. MENCHACA-ROCHA<sup>10</sup>, J. W. MITCHELL<sup>9</sup>, S. I. MOGNET<sup>3</sup>, G. NA<sup>7</sup>, S. NAM<sup>7</sup>, S. NUTTER<sup>11</sup>, I. PARK<sup>7</sup>, A. PUTZE<sup>4</sup>, E. S. SEO<sup>1,2</sup>, J. WU<sup>1</sup>, J. YANG<sup>7</sup>,

<sup>1</sup>*Institute of Physical Science and Technology, University of Maryland, College Park, Maryland, 20742, USA*

<sup>2</sup>*Department of Physics, University of Maryland, College Park, Maryland, 20742, USA*

<sup>3</sup>*Department of Physics, Penn State University, University Park, PA 16802, USA*

<sup>4</sup>*Laboratoire de Physique Subatomique et de Cosmologie, Grenoble, France*

<sup>5</sup>*Center d'Etude Spatiale des Rayonnements, UFR PCA-CNRS-UPR 8002, Toulouse, France*

<sup>6</sup>*Department of Physics, Ohio State University, Columbus, OH 43210, USA*

<sup>7</sup>*Department of Physics, Ewha Womans University, Seoul 120-750, Republic of Korea*

<sup>8</sup>*Astrophysics Space Division, NASA Goddard Space Flight Center, Greenbelt, MD 20771, USA*

<sup>9</sup>*CRESST/USRA, Columbia, MD 21044, USA*

<sup>10</sup>*Instituto de Fisica, Universidad Nacional Autonoma de Mexico, Mexico*

<sup>11</sup>*Department of Physics, Northern Kentucky University, Highland Heights, KY 41099, USA*

ysy@umd.edu

DOI: 10.7529/ICRC2011/V06/1109

**Abstract:** The primary cosmic-ray elemental spectra have been measured by the balloon-borne Cosmic Ray Energetics And Mass (CREAM) instrument. CREAM has flown six times over Antarctica since 2004. The CREAM-III payload, comprised of a tungsten/scintillating fiber calorimeter, silicon charge detector (SCD), Cherenkov camera, and timing charge detector, flew for 29 days during the 2007-2008 Antarctic season. The flight accumulated significantly more calorimeter data than the two previous flights at lower energies due to a lower electronics noise level of the calorimeter and improved read-out electronics with 16-bit analog-digital conversion. The SCD provided better resolution with reduced electronics noise than for the CREAM-I flight data. In addition, two silicon layers in the SCD provided two independent charge measurements. Charge identification with the two independent charge measurements is included in this analysis, as are estimates of efficiencies, backgrounds, and energy conversion using updated Monte Carlo (MC) simulations (with the CREAM-III flight detector configuration). These refinements had not been included in previously reported results. Proton and helium energy spectra from CREAM-III flight are presented.

**Keywords:**

## 1 Introduction

Cosmic Ray Energetics And Mass is a balloon-borne experiment to measure cosmic-ray elemental spectra using ultra long duration balloon flights in Antarctica [1]. The instrument is capable of precise charge and energy measurements of elemental spectra from  $Z = 1 - 26$  over the energy range  $\sim 10^{11} - 10^{15}$  eV.

The CREAM instrument has flown six times over Antarctica since 2004. Elemental spectra from the first two CREAM flights were reported in Ahn *et al.* (2007, 2009, 2010) and Yoon *et al.* (2011) [2, 3, 4, 5]. In particular, spectral hardening in heavy nuclei over 200 GeV/n, reported by CREAM [4], was confirmed for proton and helium spectra by the Payload for Antimatter Matter Exploration and

Light-nuclei Astrophysics [6]. More measurements above TeV can address whether this hardening spectra will roll off above  $\sim 100$  TeV or not, which many models suggest may be the energy limit of shock acceleration [7].

During the third CREAM flight, significantly more calorimeter data were accumulated than for the two previous flights at lower energies due to lower trigger threshold [8]. This improved proton and helium spectra with increased statistics. Preliminary proton and helium spectra were reported at a previous conference [9]. The charge identification method was updated and event selection for the calorimeter calibration was refined. In this paper, proton and helium spectra and updated data analysis processes are presented.

## 2 CREAM-III Instrument and Flight

The CREAM-III instrument consisted of five sub-detectors: a tungsten/scintillating fiber calorimeter, a dual layer SCD, Cherenkov Camera (CherCam), Cherenkov Detector, and a Timing Charge Detector (TCD), as shown in Figure 1. The calorimeter measures the energy of incident nuclei that interact in graphite targets located directly above it. The calorimeter is comprised of a stack of 20 tungsten layers with an overall 20 radiation lengths ( $X_0$ ) depth and 20 layers of scintillating fibers. The dual layer SCD, CherCam, and TCD provide charge identification of incident particles by measuring  $dE/dx$  in the silicon layer, Cherenkov radiation, and  $dE/dx$  in the plastic scintillator, respectively. The dual layer SCD (top and bottom SCD) provides two independent charge measurements with a resolution of  $\sim 0.2 e$  for p and He. They are segmented into pixels with an area of  $2.12 \text{ cm}^2$  each to minimize hits from back-scattered particles. More details about individual sub-detectors can be found elsewhere ([8, 11, 12, 13]). In this analysis for proton and helium spectra, an energy measurement from the calorimeter and two independent charge measurements from top and bottom SCD are used, while previous CREAM-III preliminary results were based on charge measurements from a single layer (top layer) of the SCD.

The CREAM-III payload was launched from Williams field near McMurdo station, Antarctica on December 19, 2007 and the payload landed on January 17, 2008 after  $\sim 29$  days of flight. Throughout the CREAM-III flight, detectors performed stably. For the calorimeter, no in-flight adjustments were needed for values such as the high voltage for the hybrid-photo-diodes or trigger threshold, while those were adjusted in the previous two flights to optimize data rates. The live-time fraction during data collection was about 99%. The reduced noise level in the calorimeter electronics allowed the trigger thresholds to be lowered to about 15 MeV, whereas it has been about 50 MeV for the two previous flights. In addition, the sparsification threshold



Figure 1: CREAM-III Instrument; From the top: TCD, CD, CherCam, top and bottom SCD, and Calorimeter.

value (STV) in each calorimeter channel, which suppresses the pedestal, was lowered to about  $2 \sigma$  of the pedestal.

## 3 Data Analysis

After preliminary proton and helium spectra from the CREAM-III flight were reported [9], MC simulations were generated with the CREAM-III detector configuration. Also, the event selection methods in calibration beam data analysis were modified to have more events in low gain channels. In addition, telemetry and archived flight data event selection was improved.

### 3.1 Calorimeter Calibration

The conversion factor from analog-to-digital converter (ADC) units to MeV in each channel was estimated by comparing the beam data signals with MC simulation results. Previously, the ribbon position with maximum signal was estimated in each layer. When that ribbon position was matched with the expected position, the maximum signal was used for the distribution of expected position. In this way, some channels in a layer did not have enough events due to low gain or unstable neighboring channels.

In the new event selection method, the ribbon position with maximum signal was estimated with accumulated signals of all layers in an event instead of estimating this in each layer separately. Several channels with lower gain than neighboring channels showed signal distributions. The channels with low gains have a higher calibration factor than other channels and the stability of those channels was checked during the flight. Calibration factors in most channels were not affected by this change although several channels showed a slight change due to increased events.

### 3.2 Flight Data Improved Selection

During the flight, all calorimeter events and some fraction of calibration events were transferred to the Science Operation Center in order to fit within the limited bandwidth. Since all the calibration events were archived to disk on the instrument, transferred data and archived data were merged after the flight.

Some events lost due to missing packets owing to bad satellite connections were reconstructed with stored packets. Furthermore, duplicated events caused by play-back were removed. Play-back is a scheme for re-sending data to account for missing or lost data time ranges, including some margins during the flight.

The merged telemetry data was about 8.3 GB and the amount of merged data was about 24 GB. After merging data, about 4% of calorimeter events were duplicates and thus removed. The number of collected calorimeter events was  $1.23 \times 10^6$ .

### 3.3 MC Simulations

MC simulations are mainly used for estimation of efficiencies, backgrounds, secondary effects and energy conversion matrices. The MC simulation results, based on GEANT/FLUKA 3.21 [14, 15], were generated with the CREAM-III detector configuration, while MC simulations with the CREAM-I detector configuration were used in the previous analysis. The CherCam was placed above the top SCD in the CREAM-III instrument while the Transition Radiation Detector (TRD) had been above the SCD for CREAM-I. The CherCam had greater material thickness ( $\sim 12 \text{ g/cm}^2$ ) than the TRD in CREAM-I ( $\sim 7.6 \text{ g/cm}^2$ ) and event interactions above the SCD are slightly increased, as expected.

Since the CREAM-III calorimeter had a lower energy threshold than for previous flight results, the MC simulations were generated at a lower energy ( $\sim 100 \text{ GeV}$ ) than MC simulations for CREAM-I ( $\sim 1 \text{ TeV}$ ). Efficiencies and backgrounds were estimated at several fixed energies and energy bins with scaled simulation results.

### 3.4 Charge Measurements

The two independent charge measurements from the top and bottom SCD layers during the flight are shown in Figure 2.

The charge of incident particle,  $Z$ , was defined with charges from the top and bottom SCD layers,  $Z_{tSCD}$  and  $Z_{bSCD}$ , as follows,

$$Z = \sqrt{\frac{1}{2}(Z_{tSCD}^2 + Z_{bSCD}^2)}, \quad (1)$$

where the top or bottom SCD charge,  $Z_{tSCD}$  or  $Z_{bSCD}$ , is obtained by normalizing to a signal generated by a minimum ionization particle. The measured top or bottom SCD signal was corrected to that of a vertical path-length inside the sensor to account for the incident angle.

### 3.5 Energy Measurements and Spectral Deconvolution

Deposited ADC signals were converted to a deposited energy using calibration factors in each channel. The energy measurement procedure is the same as the one used in obtaining the preliminary results, but a spectral deconvolution was used to get the incident energy distribution in this analysis, instead of using a simple conversion using a conversion factor [5].

Entries in deposited energy bins are deconvolved to incident energy bins using matrix relations. The counts  $N_{inc,i}$  in the incident energy bin  $i$  are estimated from the measured counts  $N_{dep,i}$  in deposited energy bin  $j$  by the relation,

$$N_{inc,i} = \sum_j P_{i,j} \cdot N_{dep,j}, \quad (2)$$

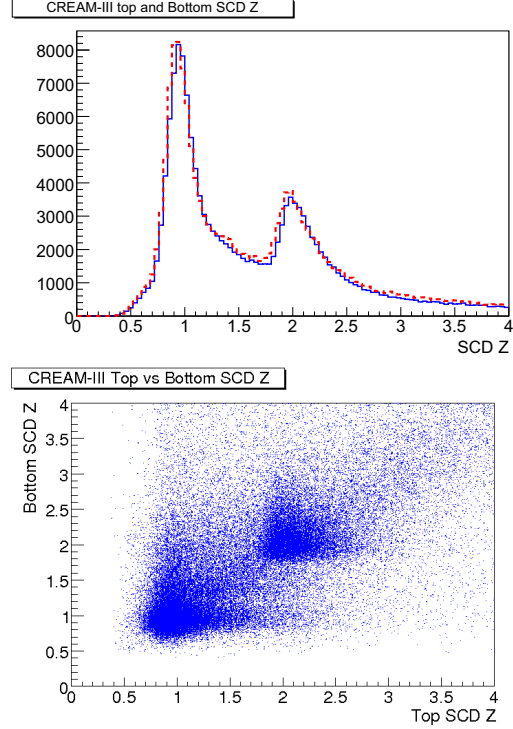


Figure 2: (top) Charge distributions of top (red dashed line) and bottom (blue solid line) SCD and (bottom) their scatter plot.

where the matrix element  $P_{i,j}$  is the probability that the events in the deposited energy bin  $j$  are from incident energy bin  $i$ . The matrix elements  $P_{i,j}$  are estimated with MC simulations with the CREAM-III detector configuration. MC simulations for helium nuclei and heavy nuclei were generated with FRITIOF/RQMD/DPMJET-II interfaced to the GEANT/FLUKA 3.21 hadronic simulation package (see Yoon *et al.* [5] for references and more details).

### 3.6 Absolute Flux

The differential flux ( $F$ ) at the top of the atmosphere in each energy bin with size  $\Delta E$  is given by

$$F = \frac{N_{inc}}{\Delta E \cdot GF \cdot \varepsilon \cdot T \cdot \eta}, \quad (3)$$

where  $N_{inc}$  is the number of events in the incident energy bin,  $GF$  is the geometry factor,  $\varepsilon$  is the efficiency,  $T$  is the live-time, and  $\eta$  is the correction for losses in the atmosphere.

Most of values used absolute flux calculations were updated due to new MC simulations and the charge selection method change. Efficiencies and backgrounds were estimated with MC simulations with the CREAM-III detector configuration. The geometry factor was estimated for particles passing through the active area of the top and bottom

SCD layers and the calorimeter area. The charge selection efficiency using top and bottom SCD layers was included in this analysis.

## 4 Results

The proton and helium spectra will be presented at the conference.

### Acknowledgment

This work was supported in the U.S. by NASA grants NNX08AC11G, NNX08AC15G, NNX08AC16G and their predecessor grants, in Korea by the Creative Research Initiatives of MEST/NRF, in France by IN2P3, CNRS, and CNES. The authors thank the NASA Wallops Flight Facility, the Columbia Scientific Balloon Facility, the National Science Foundation Office of Polar Programs, and Raytheon Polar Services Company for the successful balloon launch, flight operations, and payload recovery.

### References

- [1] Seo, E.S. *et al.* Adv. Spa. Res., 2004, **33**(10): 1777-1785
- [2] Ahn, H.S. *et al.* Astroparticle Physics, 2008, **30**(3): 133-141
- [3] Ahn, H.S. *et al.* ApJ, 2009, **707**(1): 593-603
- [4] Ahn, H.S. *et al.* ApJ Letter, 2010, **714**(1): L89-L93
- [5] Yoon, Y.S. *et al.* ApJ, 2011, **728**(2): 122
- [6] Adriani, O. *et al.* Science, 2011, **332**(6025): 69
- [7] Lagage, P.O., Cesarsky, C.J., A&A, 1983, **125**(2): 249-257
- [8] Lee, M.H. *et al.* IEEE Trans. Nucl. Sci., 2009, **56**(3): 1396-1399
- [9] Yoon, Y.S. *et al.* Int. Cosmic Ray Conf., 2009, submitted
- [10] Ahn, H.S. *et al.* Nucl. Inst. Meth. A, 2007, **579**(3): 1034-1053
- [11] Park, I.H. *et al.* Nucl. Inst. Meth. A, 2007, **570**(2): 286-291
- [12] Ahn, H.S. *et al.* Nucl. Inst. Meth. A, 2009, **602**(2): 525-536
- [13] Sallaz-Damaz, Y. *et al.* Nucl. Inst. Meth. A, 2008, **595**(1): 62-66
- [14] Brun, R.F. *et al.* , GEANT User Guide, 1984
- [15] Fasso, A. *et al.* , Proc. of IV Int. Conf. of Calorimetry in High-Energy Physics, La Biodola, Sept 20-25, 1993: 493-502